Oxygenation state of hemoglobin defines dynamics of water molecules in its vicinity

Latypova, Larisa ; Barshtein, Gregory ; Puzenko, Alexander ; Poluektov, Yuri ; Anashkina, Anastasia ; Petrushanko, Irina ; Fenk, Simone ; Bogdanova, Anna ; Feldman, Yuri

Abstract: This study focuses on assessing the possible impact of changes in hemoglobin (Hb) oxygenation on the state of water in its hydration shell as it contributes to red blood cell deformability. Microwave Dielectric Spectroscopy (MDS) was used to monitor the changes in interactions between water molecules and Hb, the number of water molecules in the protein hydration shell, and the dynamics of pre-protein water in response to the transition of Hb from the tense (T) to the relaxed (R) state, and vice versa. Measurements were performed for Hb solutions of different concentrations (5 g/dl-30 g/dl) in phosphate-buffered saline buffer. Cole-Cole parameters of the main water relaxation peak in terms of interactions of water molecules (dipole-dipole/ionic dipole) during the oxygenation-deoxygenation cycle were used to analyze the obtained data. The water mobility-represented by as a function of ln -differed dramatically between the R (oxygenated) state and the T (deoxygenated) state of Hb at physiologically relevant concentrations (30 g/dl-35 g/dl or 4.5 mM-5.5 mM). At these concentrations, oxygenated hemoglobin was characterized by substantially lower mobility of water in the hydration shell, measured as an increase in relaxation time, compared to deoxyhemoglobin. This change indicated an increase in red blood cell cytosolic viscosity when cells were oxygenated and a decrease in viscosity upon deoxygenation. Information provided by MDS on the intraerythrocytic water state of intact red blood cells reflects its interaction with all of the cytosolic components, making these measurements powerful predictors of the changes in the rheological properties of red blood cells, regardless of the cause.

DOI: https://doi.org/10.1063/5.0023945

The Journal of Chemical Physics

Oxygenation state of hemoglobin defines dynamics of water molecules in its vicinity

Cite as: J. Chem. Phys. **153**, 135101 (2020); https://doi.org/10.1063/5.0023945
Submitted: 03 August 2020 . Accepted: 16 September 2020 . Published Online: 07 October 2020

Larisa Latypova, Gregory Barshtein, Alexander Puzenko, Yuri Poluektov, Anastasia Anashkina, Irina Petrushanko, Simone Fenk, Anna Bogdanova, and Yuri Feldman

The Journal of Chemical Physics ARTICLE scitation.org/journal/jcp

Oxygenation state of hemoglobin defines dynamics of water molecules in its vicinity

Cite as: J. Chem. Phys. 153, 135101 (2020); doi: 10.1063/5.0023945
Submitted: 3 August 2020 • Accepted: 16 September 2020 •
Published Online: 7 October 2020

Larisa Latypova,[1,2] Gregory Barshtein,[3] Alexander Puzenko,[1] Yuri Poluektov,[4] Anastasia Anashkina,[4] Irina Petrushanko,[4] Simone Fenk,[5] Anna Bogdanova,[5] and Yuri Feldman[1,a)]

AFFILIATIONS

[1]Department of Applied Physics, The Hebrew University of Jerusalem, Givat Ram 91904, Israel
[2]Department of Physics, Kazan Federal University, 18 Kremlewskaya St., 420008 Kazan, Russia
[3]Department of Biochemistry, The Faculty of Medicine, The Hebrew University, Campus Ein Kerem, Jerusalem 91120, Israel
[4]Engelhart Institute of Molecular Biology, Russian Academy of Science, Vavilov St. 32, 119991 Moscow, Russia
[5]Red Blood Cell Research Group, Institute of Veterinary Physiology, University of Zürich, Winterthurerstrasse 260, CH-8057 Zürich, Switzerland

[a)]**Author to whom correspondence should be addressed:** yurif@mail.huji.ac.il

ABSTRACT

This study focuses on assessing the possible impact of changes in hemoglobin (Hb) oxygenation on the state of water in its hydration shell as it contributes to red blood cell deformability. Microwave Dielectric Spectroscopy (MDS) was used to monitor the changes in interactions between water molecules and Hb, the number of water molecules in the protein hydration shell, and the dynamics of pre-protein water in response to the transition of Hb from the tense (T) to the relaxed (R) state, and vice versa. Measurements were performed for Hb solutions of different concentrations (5 g/dl–30 g/dl) in phosphate-buffered saline buffer. Cole–Cole parameters of the main water relaxation peak in terms of interactions of water molecules (dipole–dipole/ionic dipole) during the oxygenation–deoxygenation cycle were used to analyze the obtained data. The water mobility—represented by α as a function of $\ln\tau$—differed dramatically between the R (oxygenated) state and the T (deoxygenated) state of Hb at physiologically relevant concentrations (30 g/dl–35 g/dl or 4.5 mM–5.5 mM). At these concentrations, oxygenated hemoglobin was characterized by substantially lower mobility of water in the hydration shell, measured as an increase in relaxation time, compared to deoxyhemoglobin. This change indicated an increase in red blood cell cytosolic viscosity when cells were oxygenated and a decrease in viscosity upon deoxygenation. Information provided by MDS on the intraerythrocytic water state of intact red blood cells reflects its interaction with all of the cytosolic components, making these measurements powerful predictors of the changes in the rheological properties of red blood cells, regardless of the cause.

I. INTRODUCTION

Physiological properties of red blood cells (RBCs), such as deformability, metabolic activity, and oxygen transport capacity, are tightly controlled by hemoglobin (Hb), which makes up 97% of the dry weight of the cell, and by intracellular water that makes up around 67%–69% of a RBC's total weight.[1] In healthy human beings, the mean corpuscular hemoglobin concentration ranges between 320 g/l and 360 g/l,[2] close to their solubility threshold. Therefore, interactions between the two principal components of a RBC, water and Hb, are particularly important in defining protein dynamics. The proportion between free and bound water defines the water dynamics, and thus the diffusion of gases, ions, metabolites, and other cytosolic components. It also defines the cytosolic viscosity and deformability of red blood cells that are so crucial for O_2 delivery from the lungs to peripheral organs.

The interaction of Hb with water has been studied since the first high-resolution crystal structures of oxy-, deoxy-, and met-Hb were obtained. The amount of water that was found to be

unavailable as a solvent for diffusible electrolytes was estimated as 0.3[3] or 0.45[4] g/g protein.[5] Based on the calculations, it was suggested that water may form two layers adjacent to the 150 charged groups localized at the water–Hb interface of oxyHb.[5] These assumptions were later confirmed experimentally for aqueous Hb solution at a concentration of 271 g/l.[4] Using the nuclear magnetic relaxation technique, two layers of water surrounding oxyHb were identified—one exhibiting fast exchange and one with slow exchange rate.[6] Moreover, the state of water was suggested to have an impact on the balance between the R (oxygenated) and T (deoxygenated) conformations of the Hb molecule.[7] Whether the changes in the Hb state (T–R transition, carboxylation, nitrosylation, glutathionylation, and oxidation to metHb formation) cause the alterations in the state and dynamics of the water in RBCs remains unclear. Among the methodologies used to assess the state of water in living cells, dielectric spectroscopy (DS),[4,8–10] nuclear magnetic resonance (NMR),[11] and differential scanning calorimetry (DSC)[12] are the most common, along with molecular dynamic simulation.[13] Early on, DS revealed the changes that occur in the state of water in RBCs during storage in a blood bank.[14,15] The broadening parameter of the main dielectric peak of cytosol water showed a linear dependence with the storage time, predicting the RBC deformability and longevity in circulation (see Fig. 1, blue and red symbols for two independent donors).[16] This observation was recently supported by Petrovic *et al.*,[11] who monitored the changes of intracellular water dynamics [during packed RBC (PRBC) cold storage] by H^1 NMR. Note that the broadening parameter α (dipole matrix interaction,[17] blue and red circles in Fig. 1) shows a perfect correlation with the spin–lattice relaxation time T1 (black line in Fig. 1). The authors assigned the decline of T with time of storage to the accumulation of metHb in the PRBCs.[11] In addition to oxidation, storage of PRBCs is associated with an elevation of the oxyHb/deoxyHb ratio.[18–20]

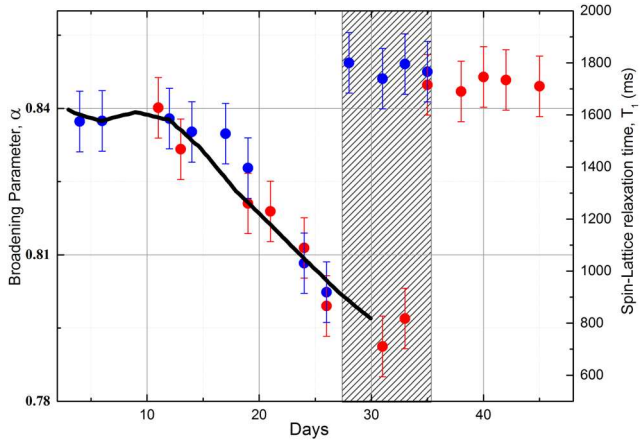

FIG. 1. The experimental relaxation times τ and the broadening parameter α for one cell during a period of 45 days of cold storage for two different samples (red and blue circles).[16] The black line corresponds to the spin–lattice relaxation time (T_1) measured over a 30-day period by Petrovic *et al.*[11] Red and blue circles are the broadening parameter α for the two different donors. The shaded rectangle indicates the region where drastic changes with RBCs occur.

The gradual increase in oxyHb in stored cells is caused by a depletion of 2,3-diphosphoglycerate, an allosteric modulator that binds to Hb and stabilizes its T conformation, thereby decreasing the Hb O_2 affinity.[21,22] Using the quartz crystal microbalance (QCM) method,[7] oxyHb was reported to bind 60 water molecules more per molecule of Hb than deoxyHb. Thus, the transition from the T to the R state could theoretically contribute to an increase in cytoplasmic viscosity, a decrease in deformability with membrane loss through vesiculation, and changes in the RBC water content.

In contrast to these predictions, acute deoxygenation of intact RBCs was suggested to cause a decrease in deformability that could not be attributed to the acute changes in the cell volume or mean corpuscular hemoglobin concentration.[23] To resolve this discrepancy, our study was designed to assess the changes in Hb hydration and water dynamics in hydration shells triggered by transition from the T to the R state using Hb solutions in phosphate buffer as the model. Dielectric relaxation of water in aqueous solutions of Hb was monitored as a function of Hb concentration and its oxygenation state. The chosen Hb concentrations range from 5 g/dl to 30 g/dl, which covers the close-to-physiological range of Hb concentration in RBCs.[2]

II. DIELECTRIC SPECTROSCOPY. THEORETICAL PART

Most of the unique features of water may be attributed to its strong polarity and to the existence of an H-bond network in its various states. This makes dielectric spectroscopy (DS) a particularly suitable method for monitoring water in complex materials.[14,15] Traditionally, water in biological tissues has been defined as either bound or free water, depending on its proximity to neighboring ions, molecules, membranes, or other interfaces. Water forming the hydration shell of the macromolecule is considered as bounded. The remaining water in the system is defined as bulk. At room temperature (25 °C), the dielectric relaxation peak of water is localized in the microwave frequency band (0.5 GHz–50 GHz). Typically, water's relaxation peak in aqueous solutions can be described by the phenomenological Cole–Cole (CC) function,[24]

$$\varepsilon^*(\omega) = \varepsilon'(\omega) - i\varepsilon''(\omega) = \varepsilon_h + \frac{\Delta\varepsilon}{1 + (i\omega\tau)^{\alpha}} - i\frac{\sigma}{\omega\varepsilon_0}. \quad (1)$$

Here, ε' and ε'' are the real and imaginary parts of the complex permittivity, $\omega = 2\pi f$ is the cyclic frequency, and $i^2 = -1$. The parameter ε_h denotes the extrapolated high-frequency permittivity, and $\Delta\varepsilon = \varepsilon_l - \varepsilon_h$ is the relaxation amplitude (with the low-frequency permittivity limit denoted by ε_l). The parameter τ is the relaxation time, σ is a *dc* conductivity, and ε_0 is the dielectric permittivity of vacuum. The exponent α ($0 < \alpha \leq 1$) is a measure of the symmetrical broadening. In the case of bulk water, for frequencies up to 40 GHz, α can be set to 1, resulting in a Debye relaxation.[25] However, whenever water interacts with another dipolar or charged entity, a symmetrical broadening of its dispersion peak occurs and a change in the attendant relaxation time is induced (see Fig. 2).

In different complex systems, water can be considered as the dipole subsystem, while the other components may be defined as a matrix. When a number of water molecules interacts with a

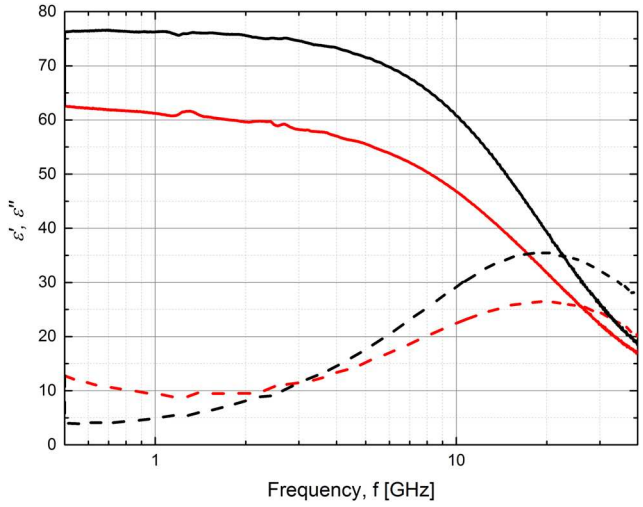

FIG. 2. Real $\varepsilon'(f)$ (solid line) and imaginary $\varepsilon''(f)$ (dashed line) parts of the complex permittivity of bulk water (black) and aqueous solution of methemoglobin (red) solutions (30 mg/dl) (red curves) at 25 °C.

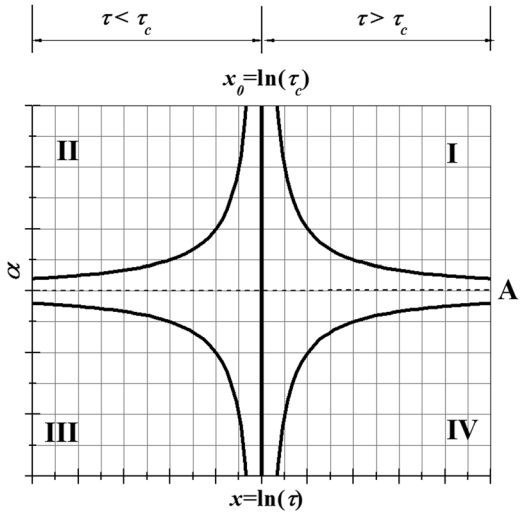

FIG. 3. The four hyperbolic branches of the function defined by Eq. (4). Reprinted with permission from A. Puzenko *et al.*, Phys. Rev. Lett. **105**, 037601 (2010). Copyright 2020 American Physical Society.

hydration center (the matrix), this interaction perturbs the structured H-bonded network of the water. Depending on the nature of the solute molecule, two types of water/matrix interactions can be distinguished: ion/dipole and dipole/dipole interactions.[26] It has been shown that the dipole/dipole interaction is accompanied by an ordering of the H-bond network of water. This assembling results in a shift of the water's main relaxation peak to the lower frequencies ("red shift"). The ion/dipole interaction, in contrast, disarrays the H-bond network of water. In this case, the water's main relaxation peak shifts to the higher frequencies ("blue shift").[26,27] The frequency band, which is usually associated with the dielectric relaxation of water in biological samples, is known as γ-dispersion and can be detected between 0.5 and 50 GHz.[28]

The broadening parameter α in Eq. (1) reflects the rate of interactions of dipole relaxation units with their surroundings and can be expressed as

$$\alpha = \frac{\ln(N_\tau/N_{0\tau})}{\ln(\tau/\tau_c)}. \tag{2}$$

This is a recursive fractal model,[17,26] where N_τ is the number of relaxations during the time interval τ, and τ_c is the cut-off time for this scaling. The elementary relaxation event, which is perceived as a single occurrence during the time τ_c, may contain a certain number $N_{0\tau}$ of relaxation acts overlapping in time, as they can occur simultaneously within the different spatial regions of the sample. Thus, the average number density of discrete interactions N_τ is described by the recursive fractal model,

$$N_\tau = N_{0\tau}\left(\frac{\tau}{\tau_c}\right)^A, \tag{3}$$

where the mass fractal dimension A adopts values in the range $0 < A \le 1$.[17]

Substituting Eq. (3) into (2) and introducing the new variables $x = \ln\tau$ and $x_0 = \ln\tau_c$, we obtain the following relationship:

$$\alpha = A + \frac{G}{x - x_0}. \tag{4}$$

Here, the parameters of the fractal model (3) are described in terms of function (4) using the simple relations,

$$N_{0\tau} = \exp(G), \quad \tau_c = \exp(x_0), \quad N_\tau = N_{0\tau}(\tau/\tau_c)^A. \tag{5}$$

In general, for a complex system with at least two components where one is a dipole subsystem,[17,29] $\alpha(\ln\tau)$ dependences may be found as described by Eq. (4). This equation demonstrates a hyperbolic curve bounded by two asymptotes, the constant A, representing the asymptotic value of the parameter α, and the asymptote $x_0 = \ln\tau_c$, dividing the full plane into two semi-planes: $\tau > \tau_c$ and $\tau < \tau_c$ (Fig. 3) The first quadrant of the plane ($\tau > \tau_c$, $\alpha > A$) represents a dipole–dipole interaction between the matrix and the bulk. The second quadrant of the plane ($\tau < \tau_c$, $\alpha > A$) represents an ion–dipole interaction. In general, for a complex system with at least two components where one is a dipole subsystem,[17,29] $\alpha(\ln\tau)$ dependences may be found as described by Eq. (5).

III. MATERIALS AND METHODS

A. Sample preparation

Lyophilized powder of human hemoglobin was obtained from Sigma Aldrich (H7379). Solutions of methemoglobin (30 g/dl, 25 g/dl, 20 g/dl, 15 g/dl, 10 g/dl, 7 g/dl, and 5 g/dl) were prepared in phosphate-buffered saline (PBS) (pH 7.4) at 25 °C to avoid changes in pH associated with changes in Hb O_2 saturation. To prepare the deoxygenated form of hemoglobin, sodium dithionite $Na_2S_2O_4$ was added in the following ratio: 10^{-4} mol hemoglobin -5×10^{-3} mol

sodium dithionite ($Na_2S_2O_4$). To prepare the oxygenated form of hemoglobin, solutions of deoxyHb were vigorously shaken while being exposed to atmospheric O_2. In order to take into account the onset of interactions between the Hb molecule hydration shells themselves, the MDS measurements were done from lower to higher Hb concentrations.

B. UV–vis analysis of hemoglobin

To monitor the state of hemoglobin in the solution, a UV–vis spectrophotometer MRC SPECTRO V-18 was used. 1 ml aliquots of oxygenated/deoxygenated solutions of hemoglobin were taken for spectroscopic measurements. UV–Vis spectra are presented in Fig. 4.

Detection of the Hb state in solution was also performed before, 5 min after supplementation of sodium dithionite causing transformation of metHb to deoxyHb, and 35 min after dithionite supplementation when reoxygenation of the deoxyHb solution was achieved by gentle swirling of the deoxyHb solution. Measurements were performed using an Avoximeter 4000 (Instrumentation Laboratory, A Werfen Company). The obtained oxy/deoxy/metHb values were similar for all concentrations tested and are shown in Table I. The rest of the Hb was represented by COHb (11.35 ± 2.06% over all measurements).

C. Microwave Dielectric Spectroscopy

Dielectric measurements were carried out in the frequency range from 500 MHz to 40 GHz using a microwave vector network analyzer (Keysight N5234B PNA-L) together with a flexible cable and slim-form probe (Keysight N1501A Dielectric Probe Kit). System calibration was performed using three references: air, a Keysight standard short circuit, and pure water at 25 °C. Calibration was supported using the E_{cal} mode. A special stand for the slim-form probe was designed and combined with a sample cell holder for liquids (total volume ~7.8 ml). The holder was temperature regulated via a thermostat connected to a Julabo CF 41 oil-based heat circulatory system. The temperature was maintained at 25 ± 0.1 °C. Each curve corresponding to oxy- and deoxyHb was measured at least six times, where each measurement took ~30 s. The real and imaginary parts $\varepsilon'(\omega)$ and $\varepsilon''(\omega)$ were evaluated using the Keysight N1500A Materials Measurement Software with an accuracy of $\Delta\varepsilon'/\varepsilon' = 0.05$ and $\Delta\varepsilon''/\varepsilon'' = 0.05$.

D. Influence of dithionite on dielectric parameters of PBS

Increasing concentrations of sodium dithionite $Na_2S_2O_4$ were used to reduce Hb and maintain it in its deoxygenated state. In order to separate the impact of Hb on the dielectric parameters from that of sodium dithionite, we assessed these parameters in Hb-free dithionite-containing PBS, in which dithionite concentrations were identical to those used for converting 10 g/dl–15 g/dl–30 g/dl MetHb to deoxyHb: [0.07M–0.14M–0.22M of sodium dithionite ($Na_2S_2O_4$)]. As follows from Fig. 5, dithionite supplementation produced a small-scale dose-dependent "blue" shift in the readouts, compared to PBS alone. However, this shift did not affect the comparison between the interaction of water with oxy and deoxyHb as both solutions contained identical concentrations of dithionite.

E. Estimation of the apolar and polar surface area of hemoglobin

Hemoglobin structures in oxygenated and deoxygenated forms were downloaded from the rcsb.org database. The structures with similar van der Waals volume and accessible surface area in and between groups were selected (oxyhemoglobin: 1LFT, 1LFV, 1GZX, 5WOG, 6BB5; deoxyhemoglobin: 2DN2, 1BIJ, 1NIH). As hemoglobin tetramer structures (2 alpha and 2 beta-subunits) in oxygenated and deoxygenated forms were superposed, we found

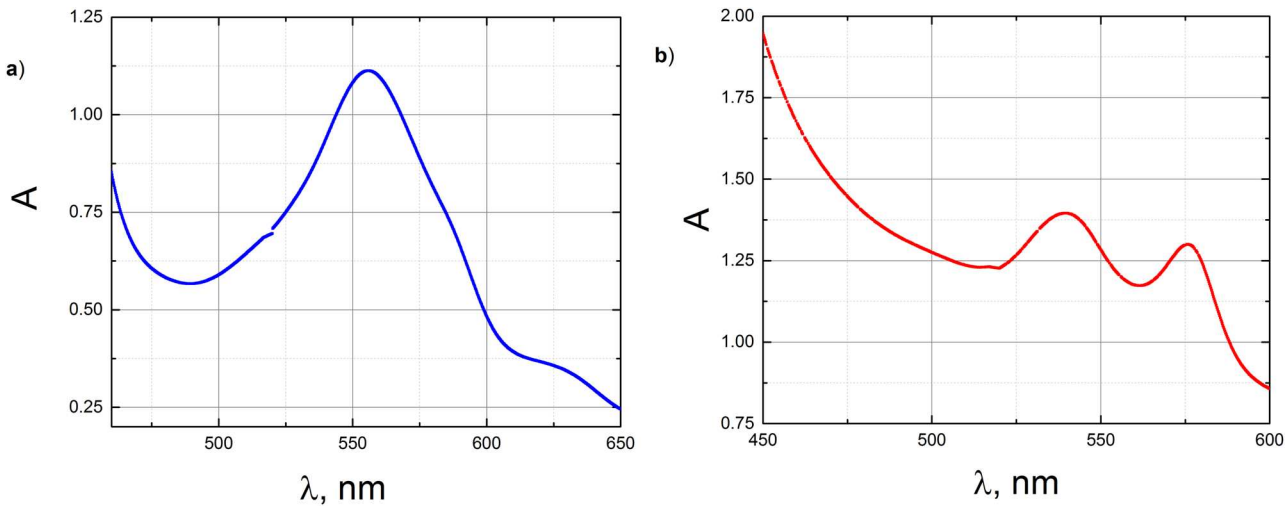

Figure. 4. UV–Vis spectra of deoxyHb (a) and oxyHb (b).

TABLE I. Time course of the Hb state induced by the addition of the reducing agent dithionite (values are shown as AVG ± SD).

Time	metHb (%)	oxyHb (%)	deoxyHb (%)
Before sodium dithionite ($Na_2S_2O_4$) supplementation	80.2 ± 0.3	4.9 ± 1.2	5.1 ± 1.9
Deoxygenation (5 min after)	14.7 ± 2.9	0	74.0 ± 2.1
Reoxygenation (35 min after)	29 ± 6.9	54.68 ± 4.3	4.4 ± 3.2

the most pronounced difference in the root-mean-square deviation (RMSD) of atomic positions for the beta-subunit of fragment 55–105. We used fragment 55–105 for further analysis. Superposition of hemoglobin structures in oxy (1lfq) and deoxy (1a3n) forms is presented in Fig. 6. The fragments have similar van der Waals volume and accessible surface area parameters. For oxyhemoglobin, it was 5139 ± 23 Å^3 and 4935 ± 21 Å^2, and for deoxyhemoglobin 5136 ± 6 Å^3 and 4943 ± 26 Å^2, respectively. Partial charges for hemoglobin fragments were calculated in the MMFF94x force field. The surfaces of the hydrophobic (apolar) and the hydrophilic (polar) area available to the solvent were calculated at pH = 7.4 in the Molecular Operating Environment (MOE) software.

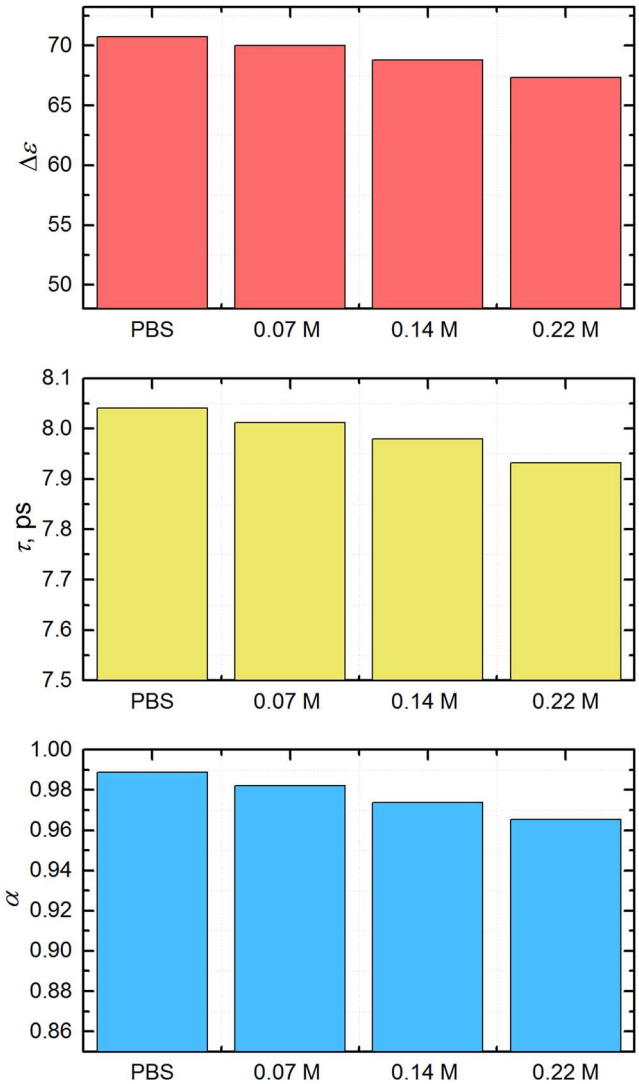

FIG. 5. Comparison of the dielectric parameters of pure PBS to PBS containing different concentrations of dithionite.

F. Statistical analysis

The comparison of data groups was performed using Student's t-test; $p < 0.05$ was considered significant. Data are presented as a means of at least three independent experiments ±SD.

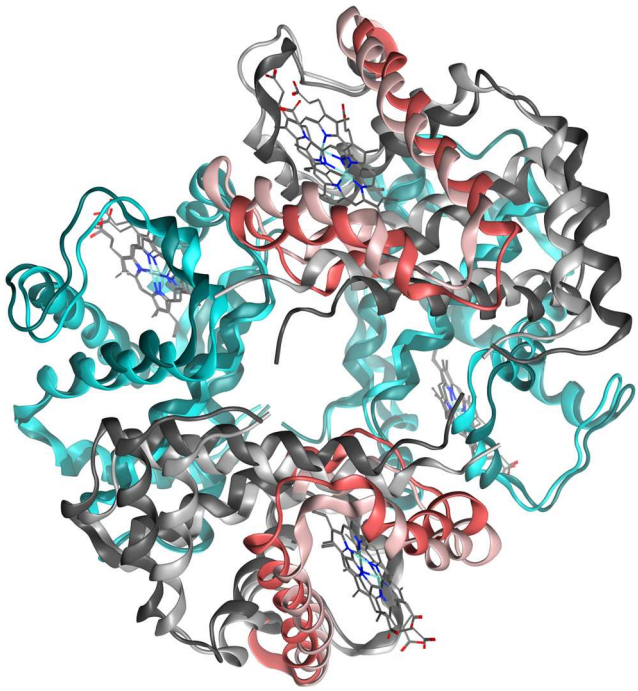

FIG. 6. Superposition of hemoglobin structures in oxy (1lfq) and deoxy (1a3n) forms. The deoxyhemoglobin alpha subunit is indicated by turquoise, and the oxyhemoglobin alpha subunit is indicated by dark turquoise. The beta-subunit of deoxyhemoglobin is shown in gray, and the beta-subunit of oxyhemoglobin in dark gray. Fragment 55–105 of the deoxyhemoglobin beta-subunit is indicated by rose, and that of oxyhemoglobin is indicated by dark rose.

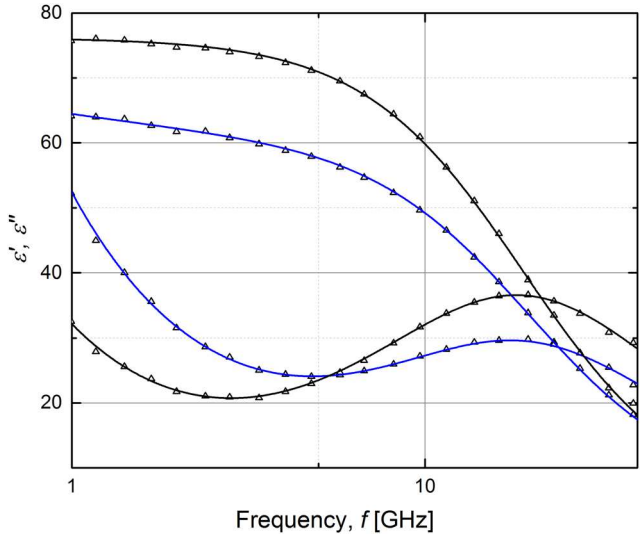

FIG. 7. The real part ε′(f) and the imaginary part ε″(f) of the dielectric spectra of PBS and aqueous solutions of deoxygenated hemoglobin (raw spectra) at a concentration of 20 g/dl at 25 °C are presented by black triangles. Fit functions of the dielectric spectra of PBS and aqueous solutions of deoxygenated hemoglobin are presented by black and blue lines, respectively.

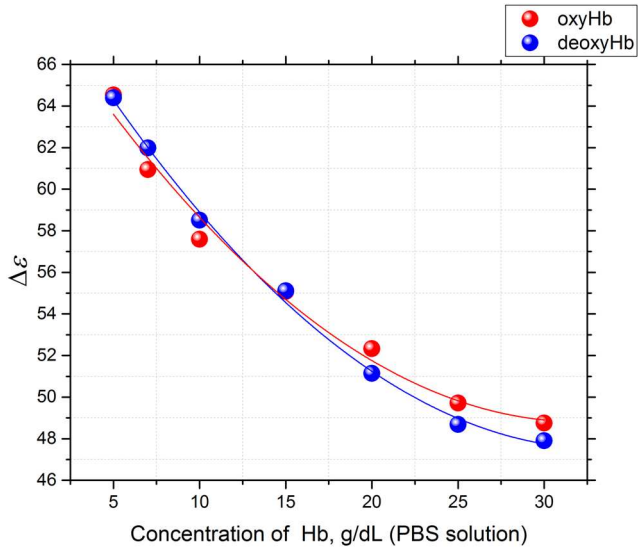

FIG. 8. The dielectric strength Δε ± 1.5% for deoxygenated (blue) and oxygenated (red) solutions of various concentrations of hemoglobin in PBS, pH = 7.4 at 25 °C.

IV. RESULTS AND DISCUSSION

The measurements of the dielectric spectrum for Hb solutions in PBS containing $Na_2S_2O_4$ were carried out at 25 °C. The spectra obtained for PBS alone and in the presence of 20 g/dl of deoxyHb solution (78%) at the frequency band 2 GHz–40 GHz are presented in Fig. 7. Dielectric spectra for four different concentrations of oxy/deoxyHb are presented in Figs. 13(a) and 13(b) in Appendix A. The spectra were fitted with Eq. (1) (combination of CC function and conductivity term) using an in-house fitting software Datama[30] applying the same routine as in our recent research on MetHb solution.[31]

The concentration dependence of the fitting parameters (relaxation time τ, broadening parameter α, and dielectric strength Δε) for both deoxygenated and oxygenated states of Hb is shown in Figs. 8, 9(a), and 9(b) and Table I (see Appendix B). The dielectric strength

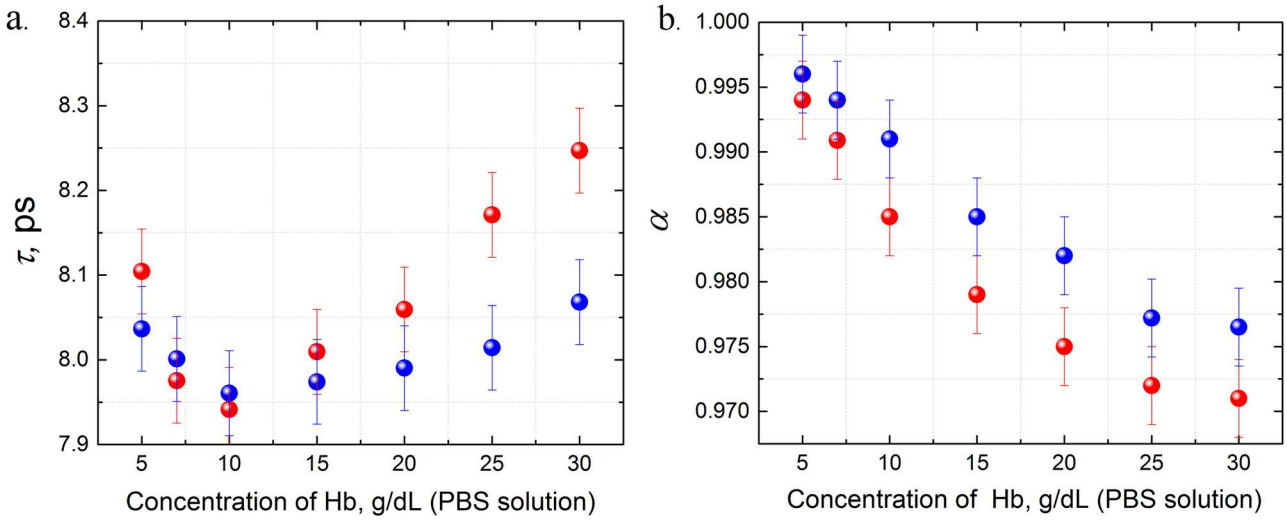

FIG. 9. The relaxation time τ (a) ±0.3%, the broadening parameter α (b) ±0.7% for deoxygenated (blue) and oxygenated (red) solutions of various concentrations of hemoglobin in PBS, pH = 7.4 at 25 °C.

Δε showed a dose-dependent decrease with increased concentrations for both states of Hb, reflecting the drop in the contribution of the bulk water in protein solution (see Fig. 8). Dielectric strength typically provides information about the structure of a solute. Since the difference in Δε for oxyHb and deoxyHb is modest, one can expect an equally minor variance in the number of hydration water molecules for both conformations.

While both the dielectric strength Δε (Fig. 8) and the broadening parameter α [Fig. 9(b)] decreased monotonically for both T and R conformations of Hb, the relaxation time had a distinct minimum at 10g/dl Hb, independent of the oxygenation state [Fig. 9(a)]. Furthermore, the dose-dependent changes in the slope of the relaxation time differed markedly between the oxyHb and deoxyHb. The evident minimum of the concentration dependence of τ attests to the competition between ion–dipole and dipole–dipole interactions in the system.

Starting from the 10g/dl concentration, the dose-dependent growth of τ of oxyHb exceeded that of deoxyHb. This indicated the more pronounced dose-dependent "red shift" that is consistent with a stronger influence of the dipole–dipole interaction of water dipoles with the solute.[26] The initial "blue shift" of the main relaxation water peak at low Hb concentrations takes place mostly due to the significant impact of the buffer ions.

Analysis of the change in polarity of the Hb molecule associated with the transition from the T to the R state was performed based on the crystal structures available in the library Protein Data Bank (rcsb.org) using MOE for calculation of the surface of hydrophobic (apolar) and the hydrophilic (polar) area available to the solvent. It was estimated for the fragment with most pronounced difference between oxyHb and deoxyHb (55–105 aa of beta-subunit) (Fig. 6). It was shown that the solvent accessible apolar surface area of the deoxy (T) state is smaller compared to that of the oxy (R) state [see Fig. 10(a)]. On the contrary, the surface area of the polar groups is larger in the deoxy state than in oxyHb [Fig. 10(b)]. The observed prolongation of the relaxation time for oxyHb compared with the deoxy form is due to the difference in the surface area of the apolar groups. Indeed, Findlay[32] has shown that the protein's hydrophobic groups impede the motion of bulk water molecules, thereby ordering them. For our system, the prolonged relaxation time observed for oxyHb indicates that in this state, Hb is more efficient in structuring the hydration shell.

This can explain the difference in relaxation times between oxyHb and deoxyHb within the concentration range from 10g/dl to 30g/dl [see Fig. 9(a)]. OxyHb has more hydrophobic groups supporting dipole–dipole interactions [see Fig. 10(a)], so the relaxation time for water in the vicinity of oxyHb is higher than for deoxyHb. These data are in good agreement with water dynamics in the hydration shell of amphiphilic macromolecules.[33]

The dose-dependent decay of the broadening parameter α with increased Hb concentration indicates [in accordance with Eq. (2)] the differences in dipole–matrix interactions between the T and R conformations [see Fig. 9(b)]. It was shown previously that $\alpha(\ln \tau)$ dependences can resolve the type of dipole–matrix interaction and predict the onset of relaxation in aqueous solutions.[26,34] The symmetrical broadening of the main water peak and its position are the key features of the spectra (see Figs. 7 and 9). To understand

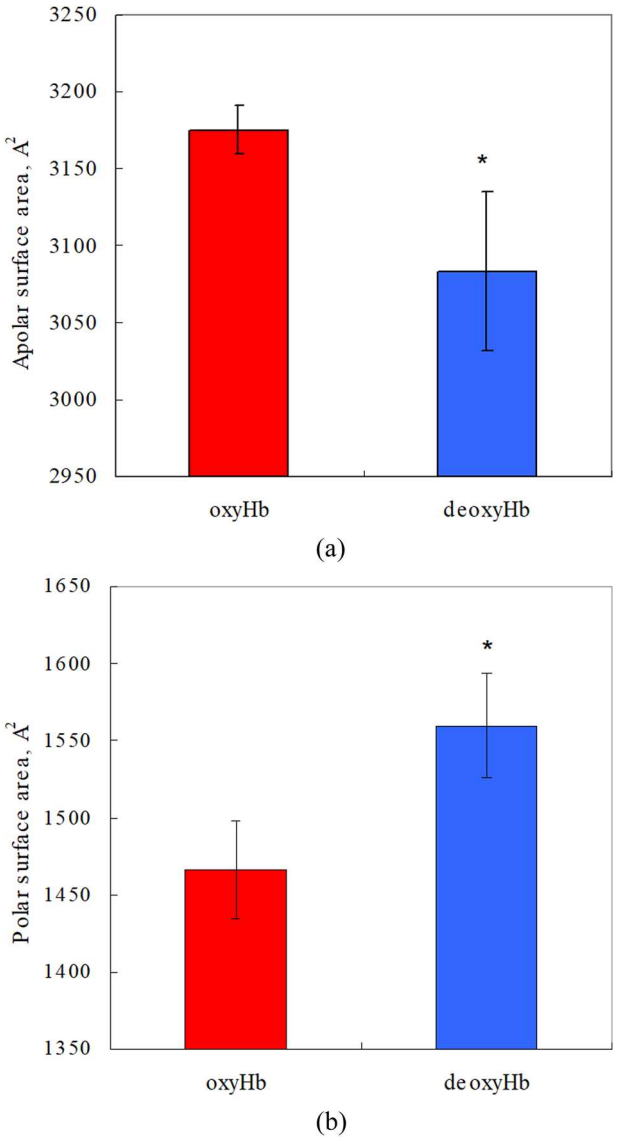

FIG. 10. The solvent accessible surface area of apolar (a) and polar (b) amino acid residues in the oxy and deoxy forms of hemoglobin. Data are presented as a means of at least three values obtained for different structures ±SD. $*p < 0.01$.

the type of interaction that occurs between the matrix (Hb macromolecule) and water dipoles, we have referred to the dependence $\alpha(\ln \tau)$ (Fig. 11).

The broadening parameter α describes the average number of discrete interactions N_τ of the dipole relaxation units with their surroundings, which occur during the time of observation (τ/τ_c) [Eq. (2)].[26] The time scale τ_c is a cutoff that defines the scaling in time $(\tau < \tau_c)$, and $N_{0\tau}$ is the average number of elementary relaxation acts happening during the time interval $[0, \tau_c]$ [see Fig. 3 and Eqs. (3) and (5)]. For both conformations of Hb, the plots $\alpha(\ln \tau)$ demonstrate similar features. The dependences $\alpha(\ln \tau)$ [see Figs. 11(a)

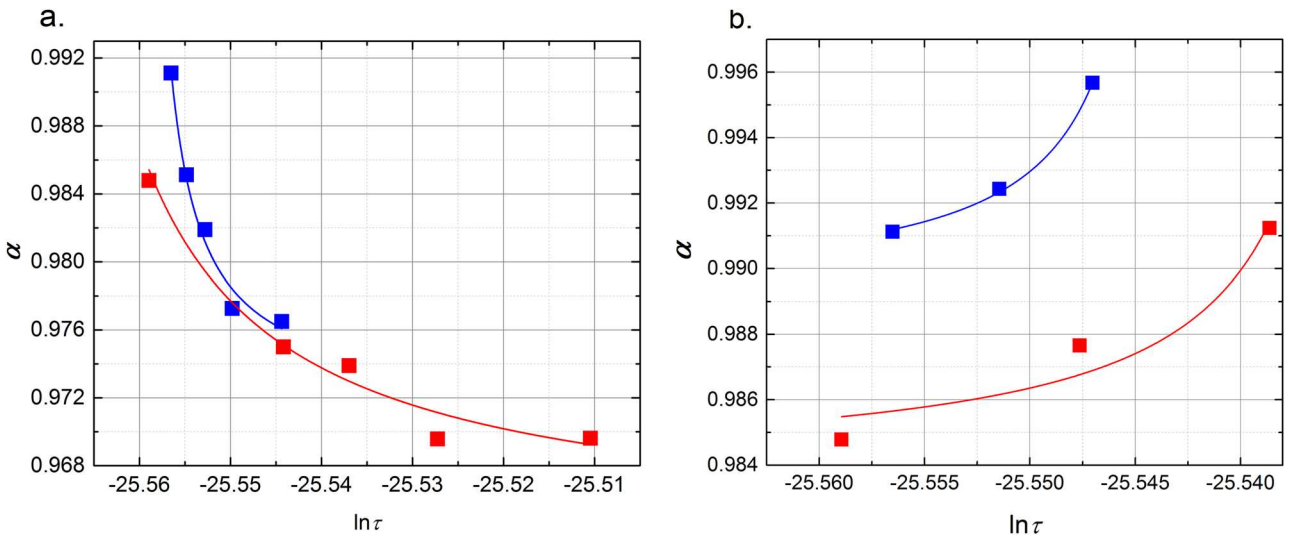

FIG. 11. $\alpha(\ln \tau)$ dependence for deoxygenated (blue) and oxygenated (red) solutions of hemoglobin at concentrations higher than 10g/dl (a) and concentrations lower than 10g/dl (b) in PBS pH = 7.4 at 25 °C.

and 11(b)] correspond to the first ($\tau > \tau_c$; $\alpha >$ A) and second ($\tau < \tau_c$; $\alpha >$ A) quadrants of the hyperbolic branches of the universal function [Eq. (4)].

The sharp transformation of the curves is observed for both states of Hb at the concentration of 10g/dl [see Figs. 11(a) and 11(b)]. At lower concentrations, the behavior of $\alpha(\ln \tau)$ corresponds to that in ionic solutions (second quadrant).[27] At high concentrations, the function $\alpha(\ln \tau)$ is moved to the first quadrant similar to monosaccharide solutions.[26] In other words, the dipole–dipole interactions are dominant at high Hb concentrations, while at low concentrations, the ion–dipole interactions between water and the PBS buffer ions prevail over the water–Hb interactions, and the corresponding curve appears in the second quadrant [see Figs. 11(a) and 11(b)]. Furthermore, both deoxyHb and oxyHb solutions are characterized by two cutoff times τ_c that correspond to different branches of Eq. (4). All values of τ_c and $N_{0\tau}$ were calculated using Eqs. (4) and (5). The values of τ_c and $N_{0\tau}$ for oxyHb and deoxyHb are presented in Table II. In the low concentration area ($\tau < \tau_c$, second quadrant), the asymptotic value τ_c approaches the values typical to the ionic solutions:[26] For deoxyHb, $\tau_c = 8.06$ ps and $N_{0\tau} \cong 1$, and for oxyHb, $\tau_c \cong 8.15$ ps and $N_{0\tau} \cong 1$. This time is slightly shorter than the relaxation time of the bulk water at this temperature. With the increase of concentration, we observe the transition of the $\alpha(\ln \tau)$ dependence for both conformations to the first quadrant ($\tau > \tau_c$), which indicates typical dipole–dipole interactions.[26,34] The asymptotic value τ_c approaches the values for deoxyHb $\tau_c = 7.92$ ps and $N_{0\tau} \cong 1$, and for oxyHb, $\tau_c \cong 7.55$ ps and $N0\tau \cong 1$. However, the range of τ_c is still significantly higher than in the case of simple nonionic solutions[26] but smaller than the relaxation of bulk water. It has recently been shown[35] that the experimental relaxation time of bulk water is associated with the minimal size of the water cluster. It means that the size of these clusters reduces in the case of Hb for T (deoxy) and R (oxy) conformations. Furthermore, the charge distribution on the protein surface in oxyHb and doxyHb defines the difference between them. Furthermore, the value $N_{0\tau} \cong 1$ for both conformations indicates a single relaxation associated with the water cluster of smaller size compared to the bulk water.

TABLE II. Values of τ_c and $N_{0\tau}$ for oxyHb and deoxyHb.

	oxyHb τ_c, ps	deoxyHb τ_c, ps	oxyHb $N_{0\tau}$	oxyHb $N_{0\tau}$
$\tau < \tau_c$	8.15	8.06	1	1
$\tau > \tau_c$	7.55	7.92	1	1

As mentioned above, the dielectric relaxation of bulk water up to 40 GHz is described well by the Debye relaxation function. One of the first models of the dielectric relaxation of water was Debye's theory where the rotation diffusion of spherical polar molecules in a viscous continuum is considered as the main mechanism of the relaxation.[36] Thus, the viscosity of the solvent η can be associated with the experimental relaxation time τ of water by the simple Debye equation,

$$\eta = \frac{\tau kT}{4\pi a^3}, \tag{6}$$

where a is the radius of a water molecule, k is the Boltzmann constant, and T is the absolute temperature. This simple relationship describes the rotational diffusion of water in the bulk only in the first approximation. The dielectric relaxation of water is more complex than a simple rotational diffusion of a single water molecule. In particular, the rotation of a water molecule occurs within an open H-bond network rather than in a viscous continuum. Therefore, today, it is suggested that water's dipole rotational dynamics reflects switching between different dipole directions rather than its continuous diffusion.[35] However, the Debye model yields the correct value for

the dielectric time relaxation obtained from the viscosity of the bulk water over a wide temperature range.[35,36] Thus, one can estimate the solvent effective viscosity of solutions of oxy- and deoxyHb using Eq. (6) (see Fig. 12). Indeed, as follows from Fig. 12, the viscosity of deoxyHb is lower than that of oxyHb within the physiologically relevant Hb concentration range (30 g/dl–35 g/dl).

For clinical and biological applications, these findings suggest that an increase in parameters, such as the mean corpuscular hemoglobin concentration, will result in a more pronounced increase in the viscosity of well-oxygenated red blood cells in the lungs than within capillaries in the hypoxic periphery. Earlier on, similar observations of advanced deformability of deoxygenated red blood cells were reported using a mouse model.[37] The authors explained the changes in deformability by a partial de-attachment of the cytoskeleton from the lipid bilayer. Our data suggest that a decrease in the viscosity of deoxyHb in the cytosol of human red blood cells could also contribute to the observed changes. The obtained data suggest that an increase in oxygenation of stored cells may (when substantial) contribute to the increase in the rigidity of the stored cells. Thus, the degree of hemoglobin oxygenation may have an impact on the cytosolic viscosity and diffusion rates in the cytosol due to the changes in the mobility of water molecules next to Hb. The presence of such a link should have the following consequences.

First, following Kramer's theory of reaction kinetics,[38,39] which relates the reaction rate to the viscosity of the solvent, it can be expected that within the oxy/deoxy cycle, changes (fluctuations) in the rates of enzymatic reactions in the erythrocyte cytoplasm should occur.

Second, following the results obtained by Longeville and Stingaciu,[40] relating oxygen capture to the mobility of the hemoglobin molecule, it can be expected that a decrease in the viscosity of water (caused by the deoxygenation of Hb) should facilitate the binding of O_2 to deoxyHb.

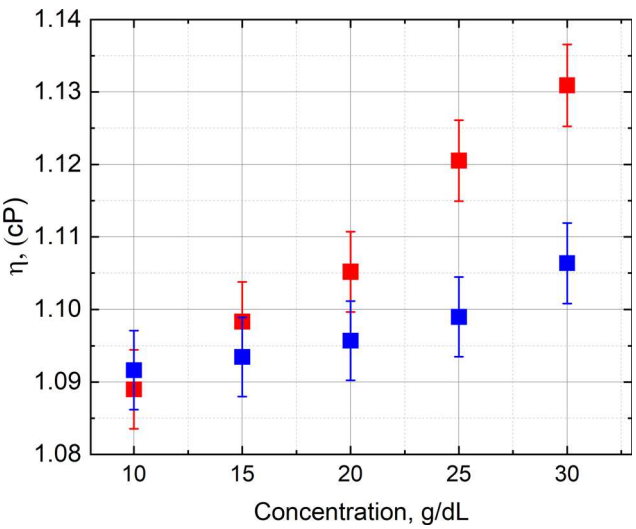

FIG. 12. Viscosity of water for deoxygenated (blue) and oxygenated (red) solutions of hemoglobin in PBS, pH = 7.4 at 25 °C.

V. CONCLUSIONS

In this work, we successfully studied the microwave dielectric response of water in Hb solutions. It was shown that MDS is sensitive to the differences in interplay between hydration and bulk water for Hb conformations in T and R states. This was the first study to show the impact of Hb oxygen saturation on the water mobility at high Hb concentrations. The biological value of this observation requires validation using intact red blood cells or whole blood, a study that is currently under way. Using MDS, the dielectric properties of cytosolic water become a powerful tool for assessing the impact of stress, disease, or drugs on red blood cell properties. In all probability, this approach will not distinguish between the impact of Hb oxygenation and changes in other cytosolic components, such as ions, metabolites, or other molecules, but it will reveal changes in the bulk water state in the cells in response to treatment. The use of parameters, such as the broadening parameter α, relaxation time τ, and dielectric strength $\Delta\varepsilon$, as prognostic and diagnostic markers requires further validation.

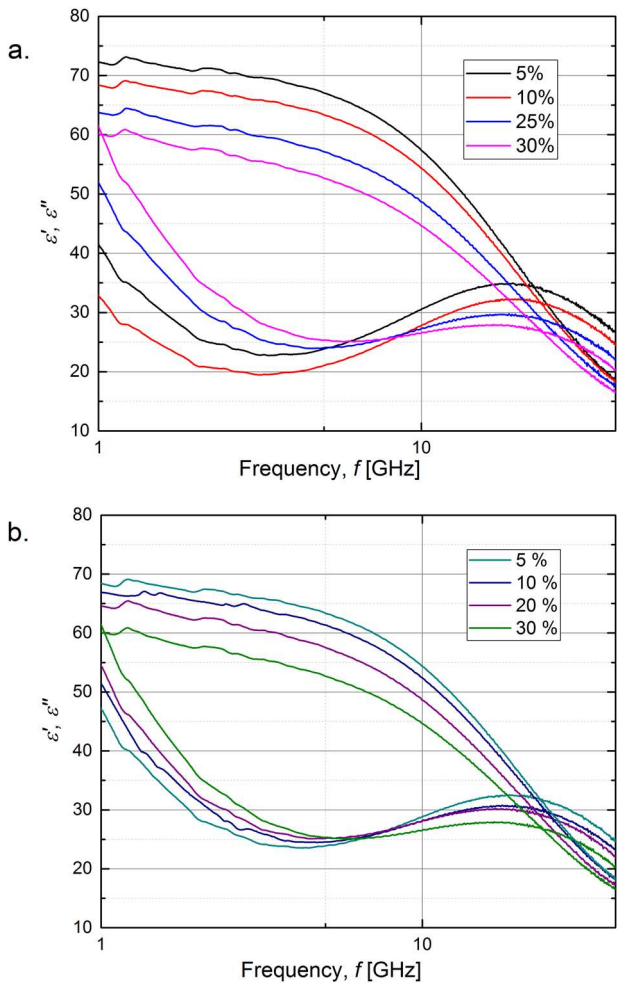

FIG. 13. Dielectric spectra for four different concentrations of deoxyHb (a) and oxyHb (b) in PBS, pH = 7.4 at 25 °C.

AUTHORS' CONTRIBUTION

All authors contributed equally to this work.

ACKNOWLEDGMENTS

The authors thank Keysight Technologies Israel Ltd. and INTERLLIGENT RF and Microwave Solutions for the loan of the Vector Network Analyzer Agilent, Grant No. N5234B PNA-L. The authors thank the Swiss National Science Foundation, Grant No. CRSII5_180234, for their financial support for the research project "Premembrane and cytosolic water as a marker of red blood cell aging *in vivo* and *in vitro*." This study was supported by the Russian Science Foundation, Grant No. 19-14-00374, for modeling simulation (Figs. 7 and 11). The authors thank ISF Grant No. 341/18 for the financial support for this research project.

There are no conflicts to declare.

APPENDIX A: DIELECTRIC SPECTRA FOR OXYGENATED AND DEOXYGENATED HEMOGLOBIN

APPENDIX B: FITTING PARAMETERS FOR OXYGENATED AND DEOXYGENATED HEMOGLOBIN.

Concentration of deoxygenated Hb (g/dl)	Δε ±1.5%	τ (ps) ±0.3%	α ±0.7%
5	64.40	8.04	0.996
7	61.99	8.00	0.994
10	58.51	7.96	0.991
15	55.11	7.97	0.985
20	51.14	7.99	0.982
25	49.51	8.01	0.977
30	47.90	8.11	0.976

Concentration of oxygenated Hb (g/dl)	Δε ±1.5%	τ (ps) ±0.3%	α ±0.7%
5	64.52	8.10	0.994
7	60.95	7.98	0.991
10	57.60	7.94	0.985
15	55.08	8.01	0.979
20	52.33	8.06	0.975
25	49.89	8.17	0.972
30	48.75	8.31	0.971

DATA AVAILABILITY

The data that support the findings of this study are available within the article.

REFERENCES

[1] R. I. Weed, C. F. Reed, and G. Berg, J. Clin. Invest. **42**, 581 (1963).
[2] C. Chernecky and B. Berger, *Laboratory Tests and Diagnostic Procedures* (Saunders, Elsevier, Philadelphia, 2013), p. 1232.
[3] S. G. Adair and M. E. Adair, Proc. R. Soc. London, Ser. B **120**, 422 (1936).
[4] E. H. Grant *et al.*, Biochem. J. **122**, 691 (1971).
[5] J. C. Kendrew *et al.*, Nature **190**, 666 (1961).
[6] J. Brnjas-Kraljevic, G. Pifat, and S. Maricic, Physiol. Chem. Phys. **11**, 371 (1979); available at https://pubmed.ncbi.nlm.nih.gov/538101/
[7] M. F. Colombo, D. C. Rau, and V. A. Parsegian, Science **256**, 655 (1992).
[8] K. Ring *et al.*, Arch. Mikrobiol. **65**, 48 (1969).
[9] Y.-Z. Wei *et al.*, J. Phys. Chem. **98**, 6644 (1994).
[10] W. von Casimir *et al.*, Biopolymers **6**, 1705 (1968).
[11] A. Petrovic, A. Krauskopf, E. Hassler, R. Stollberger, and E. Scheurer, Forencis Sci Int **262**, 11 (2016).
[12] G. Sartor and G. P. Johari, J. Phys. Chem. B **101**, 6575 (1997).
[13] J. N. Dahanayake and K. R. Mitchell-Koch, Front. Mol. Biosci. **5**, 292 (2018).
[14] Y. Feldman *et al.*, Colloids Polym. **292**, 1923 (2014).
[15] T. Chretiennot, D. Dubuc, and K. Grenier, Sensors **16**, 1733 (2016).
[16] E. Levy *et al.*, J. Phys. Chem. B **120**, 10214–10220 (2016).
[17] A. Puzenko, P. Ben Ishai, and Y. Feldman, Phys. Rev. Lett. **105**, 037601 (2010).
[18] C. G. Atkins, K. Buckley, D. Chen, H. Georg Schulze, D. V. Devine, M. W. Blades, and R. F. B. Turner, Analyst **141**, 3319 (2016).
[19] K. Buckley *et al.*, Analyst **141**, 1678 (2016).
[20] M. Z. Vardaki *et al.*, Analyst **143**, 6006 (2018).
[21] C. Lenfant *et al.*, J. Clin. Invest. **47**, 2652 (1968).
[22] J. Monod, J. Wyman, and J. P. Changeux, J. Mol. Biol. **12**, 88 (1965).
[23] M. Uyuklu, H. J. Meiselman, and O. K. Baskurt, Clin. Hemorheol. Microcirc. **41**, 179 (2009).
[24] K. S. Cole and R. H. Cole, J. Chem. Phys. **9**, 341 (1941).
[25] P. Debye, *Polar Molecules* (Dover, New York, 1929).
[26] E. Levy *et al.*, J. Chem. Phys. **136**, 114502 (2012).
[27] E. Levy *et al.*, J. Chem. Phys. **136**, 114503 (2012).
[28] C. Gabriel, S. Gabriel, and E. Corthout, Phys. Med. Biol. **41**, 2231 (1996).
[29] Y. Feldman, A. Puzenko, and Y. Ryabov, in *Fractals, Diffusion, and Relaxation in Disordered Complex Systems: Advances in Chemical Physics, Part A* (John Wiley & Sons, New York, 2006), p. 1.
[30] N. Axelrod *et al.*, Meas. Sci. Technol. **15**, 755 (2004).
[31] L. Latypova *et al.*, J. Chem. Phys. **153**, 045102 (2020).
[32] I. Findlay *et al.*, Prog. Biophys. Mol. Biol. **96**, 482 (2008).
[33] J. Zhang, L. Liu, Y. Chen, B. Wang, C. Ouyang, Z. Tian, J. Gu, X. Zhang, M. He, J. Han, and W. Zhang, J Phys Chem B 219 4; 123(13): 2971–2977.
[34] E. Levy *et al.*, J. Chem. Phys. **140**, 135104 (2014).
[35] I. Popov *et al.*, Phys. Chem. Chem. Phys. **18**, 13941 (2016).
[36] N. Agmon, J. Phys. Chem. **100**, 1072 (1996).
[37] S. Zhou *et al.*, Sci. Adv. **5**, eaav8141 (2019).
[38] P. Sashi and A. K. Bhuyan, Biochemistry **54**, 4453 (2015).
[39] S. Uribe and J. G. Sampedro, Biol. Proced. Online **5**, 108 (2003).
[40] S. Longeville and L. R. Stingaciu, Sci. Rep. **7**, 10448 (2017).